

ABSTRACT

Bacterial transport in porous media can be affected by several factors, such as cell concentration, water velocity, and attachment onto the solid matrix or suspended in the aqueous phase soil particles (e.g. clays). Gravity, also may significantly influence bacterial transport behavior in the subsurface. The present study aims to determine the gravity effect on transport and cotransport of bacteria species *Pseudomonas (P.) putida* and kaolinite colloidal particles in porous media. Transport experiments were conducted under up-, down- and horizontal-flow conditions in water saturated columns packed with glass beads. Thus, three different flow directions, 1) against gravity (up-flow), 2) in the same direction as gravity (down-flow) and 3) perpendicular to gravity (horizontal-flow), were performed. The experimental data indicated that these three flow modes influenced in a different way the kaolinite-*P. putida* cotransport behavior as well as the attachment of bacteria onto kaolinite particles. Furthermore, theoretical interaction energy calculations suggested that the extended DLVO theory predicts bacteria attachment onto kaolinite better than the classical DLVO theory. Finally, we used moment analysis and determination of collision efficiencies to further analyze the results.

Materials and Methods

Column experiments were conducted using a glass column with a diameter of 2.5 cm and a length of 30 cm (Figure 1). A fresh column was packed for each experiment by placing glass beads with diameter 2 mm. The dry bulk density of the porous media and the porosity were determined to be $\rho_b = 1.61$ kg/L and $\theta = 0.42$. Sterile distilled dionized water was used as the influent (pH = 7 at $26 \pm 1^\circ\text{C}$). The water flow rate employed was 3 mL/min, which corresponded to an interstitial water velocity of $U = 1.46$ cm/min.

Pseudomonas putida (ATCC17453) is an aerobic, rod-shaped, gram-negative, motile bacterium, with an average diameter of 2.16 ± 0.4 μm . The diameter of kaolinite clay particles was less than 2 μm .

Transport experiments were conducted under horizontal-, up- and down-flow conditions in water saturated columns. Initial experiments were performed with bacteria and kaolinite alone in order to evaluate the effect of gravity on their individual transport characteristics. Finally, *P. putida* and kaolinite particles were injected simultaneously into the packed column in order to investigate their cotransport behavior under different flow modes.

The initial concentrations for *P. putida* and kaolinite employed, were $C_{D0} = 25$ mg/L and $C_{K0} = 150$ mg/L, respectively. Tracer experiments were conducted to characterize the porous media. Chloride, in the form of potassium chloride (1500 mg/L), was chosen as the non-reactive tracer.

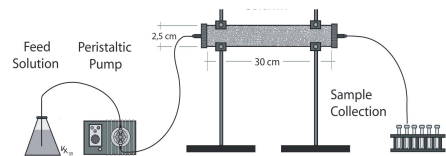


Figure 1. Picture of the experimental apparatus under horizontal-flow mode.

Theoretical considerations Moment analysis

The tracer and colloidal concentrations obtained at location $x=L$, were analyzed by the absolute temporal moments [1]:

$$m_n(x) = \int_0^\infty t^n C(x, t) dt \quad (1)$$

The normalized temporal moments are defined as:

$$M_n(x) = \frac{m_n(x)}{m_0(x)} = \frac{\int_0^\infty t^n C(x, t) dt}{\int_0^\infty C(x, t) dt} \quad (2)$$

The first normalized temporal moment, M_1 , characterizes the center of mass of the concentration distribution curve and defines the average velocity. The second normalized temporal moment, M_2 , characterizes the spreading of the concentration distribution curve. Worthy to note is that the ratio $M_{10}/M_{1(0)}$ represents the velocity of colloidal particles relative to conservative tracer. If $M_{10}/M_{1(0)} < 1$ there exists retardation of colloids and if $M_{10}/M_{1(0)} > 1$ there exists velocity enhancement of colloid particles.

The mass recovery, M_r , of the tracer or suspended particles is quantified by the following expression:

$$M_r(L) = \frac{m_\theta(L)}{C_{i0} t_p} = \frac{\int_0^\infty C_i(L, t) dt}{\int_0^\infty C_i(0, t) dt} \quad (3)$$

The corresponding $M_{10}/M_{1(0)}$ and M_r values are listed in Table 1.

Collision efficiency

The dimensionless collision efficiency, α , which is the ratio of the colloids attached to the total number of collisions between particles and collector surface (Table 1), is given by the relation [2]:

$$\alpha = -\frac{2d_c \ln\left(\frac{M_r(i)}{M_r(\text{Tr})}\right)}{3(1-\theta)n_0 L} \quad (4)$$

where d_c is the diameter of the porous media, n_0 is the single collector efficiency defined as [3]:

$$n_0 = 2.4A_s^{1/3} N_R^{-0.081} N_{Pe}^{-0.715} N_{vdW}^{0.052} + 0.55A_s N_R^{1.675} N_A^{0.125} + 0.22N_R^{-0.24} N_G^{1.11} N_{vdW}^{0.053} \quad (5)$$

where A_s is a porosity depended parameter, $N_R = d_p/d_c$, N_{Pe} is the Peclet number, N_{vdW} is the van der Waals number, N_A is the attraction number, N_G is the gravity number.

References

- Vasiliadou I.A., Chrysikopoulos C.V., Water Resour. Res. 47 (2011) W02543.
- Syngouna V.I., Chrysikopoulos C.V., Colloids Surf. A 416 (2013) 56- 65.
- Tufenkji N., Elimelech M., Environ. Sci. Technol. 38 (2004) 529-536.
- Loveland J.P., Ryan J.N., Amy G.L., Harvey R.W., Colloids Surf. A: Physicochem. Eng. Aspects 107 (1996) 205.
- Bergendahl J., Grasso D., AIChE J. 45 (1999) 475.

Sphere-Plate (sp) and Sphere-Sphere (ss) Interactions

The total interaction energy between two approaching surfaces is determined by the van der Waals, Φ_{vdW} , double layer, Φ_{dl} , and Born, Φ_{Born} , potential energies [4]:

$$\Phi_{DLVO}(h) = \Phi_{vdW}(h) + \Phi_{dl}(h) + \Phi_{Born}(h) \quad (6)$$

The extended-DLVO theory considers the additional contribution of the Lewis acid-base interaction energy, Φ_{AB} [5]:

$$\Phi_{XDLVO}(h) = \Phi_{DLVO}(h) + \Phi_{AB}(h) \quad (7)$$

For sphere-plate interactions, where a spherical (colloidal particles) surface is approaching a planar (glass beads) surface, the Φ_{AB-sp} is given by the relation:

$$\Phi_{AB-sp}(h) = 2\pi r_p \lambda_{AB} \Phi_{AB(h-h_0)} \exp\left[-\frac{h_0-h}{\lambda_{AB}}\right] \quad (8)$$

For sphere-sphere interactions, where two spherical (colloidal particles) surfaces are approaching each other, the Φ_{AB-ss} is given by the relation:

$$\Phi_{AB-ss}(h) = 2\pi \frac{r_{p1} r_{p2}}{r_{p1} + r_{p2}} \lambda_{AB} \Phi_{AB(h-h_0)} \exp\left[-\frac{h_0-h}{\lambda_{AB}}\right] \quad (9)$$

where h nm is the separation distance between the approaching surfaces, $\Phi_{AB(h-h_0)}$ is the Lewis acid-base free energy of interaction between two surfaces at $h_0 = 0.25$ nm, r_p the radius of the spherical particles, $\lambda_{AB} = 1$ nm is the decay (Debye) length of water.

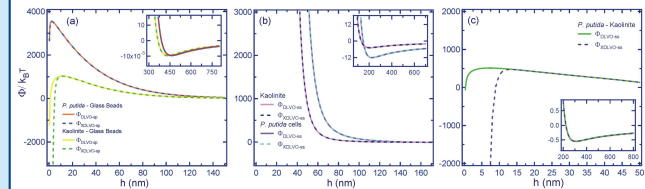


Figure 2. Predicted DLVO and XDLVO interaction energy profiles as a function of separation distance (h) among (a) *P. putida*-glass beads (sp) and kaolinite-glass beads (sp), (b) *P. putida*-*P. putida* cells (ss) and kaolinite-kaolinite particles (ss) and (c) Kaolinite-*P. putida* particles (ss).

The $\Phi_{DLVO-sp}$ and $\Phi_{XDLVO-sp}$ predicted profiles for *P. putida* (Fig. 2(a)) suggest that the conditions are highly unfavorable for irreversible bacteria attachment onto glass beads. This is in agreement with the experimental data (Table 1 and Fig. 3(a)). The acid-base interactions are only affecting the energy curve at small separation distances near the primary minimum. Therefore, the acid-base interactions were involved in the attachment of kaolinite onto glass beads (Fig. 2(a)) and of *P. putida* onto kaolinite particles (Fig. 2(c)) at the primary minimum, Φ_{min1} .

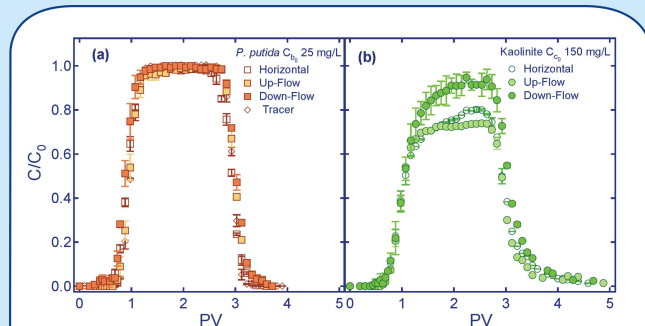


Figure 3. Experimental data for individual transport of (a) *P. putida* and (b) kaolinite under different flow modes.

Results and Discussion

The normalized breakthrough data from the individual transport and cotransport of *P. putida* and kaolinite particles for three different flow modes are presented in Figs. 3 and 4, respectively. Clearly, for both cases (transport and cotransport) the M_r of kaolinite particles (Table 1) was higher under down- than up-flow conditions. Similar results were observed for *P. putida* individual transport. Results from cotransport indicated that the *P. putida* M_r decreased during both up- and down-flow conditions compared to the horizontal mode.

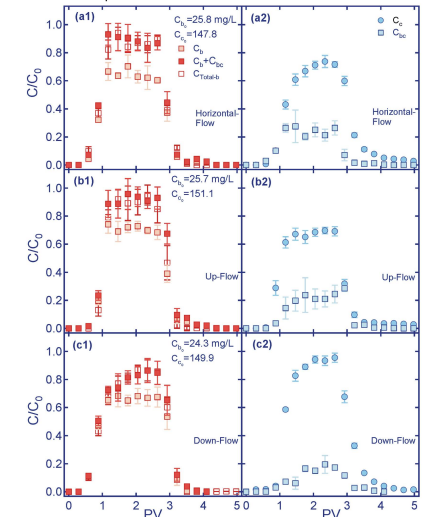


Figure 4. Experimental data for *P. putida* and kaolinite cotransport for (a) Horizontal-flow, (b) Up-flow and (c) Down-flow. Where C_c the suspended *P. putida*, C_0 the suspended kaolinite and C_{c0} the *P. putida* attached onto suspended kaolinite. The total *P. putida* was labeled as $C_{c0} + C_c$ and $C_{c,ss}$.

The calculated α values were much higher under up-flow conditions for most of the cases, indicating that the conditions were more favorable for colloidal attachment. Also, the ratio $M_{10}/M_{1(0)} > 1$ denotes that *P. putida* velocity was slightly enhanced under up-flow conditions (Table 1).

Table 1. Results obtained from the Moment analysis and Collision efficiency calculations.

Transport	Flow-Mode	M_r (%)	$M_{10}/M_{1(0)}$	$\alpha (\times 10^3)$
Tracer	Horizontal	101.3	0.98	0
	Up-Flow	102.9	1.00	0
	Down-Flow	103.8	0.99	0
<i>P. putida</i>	Horizontal	82.7	1.07	2.10
	Up-Flow	79.4	1.06	2.52
	Down-Flow	99.4	1.09	0.20
Kaolinite	Horizontal	95.0	0.97	1.00
	Up-Flow	94.4	1.02	1.10
	Down-Flow	92.8	1.00	1.36
<i>P. putida</i> total exit the column	Horizontal	79.9	0.98	3.69
	Up-Flow	75.4	1.01	4.59
	Down-Flow	78.4	0.97	3.98
<i>P. putida</i> exit the column attached	Horizontal	25.7	0.96	21.30
	Up-Flow	24.4	1.10	22.11
	Down-Flow	15.4	1.12	29.26
Kaolinite	Horizontal	76.9	1.14	2.85
	Up-Flow	73.8	1.03	3.28
	Down-Flow	97.5	1.12	0.40

Finally, the presence of kaolinite affected *P. putida* transport because the M_r of bacteria was substantially reduced (more under down-flow) in the presence of kaolinite compared to the case of individual bacterial transport. This phenomenon may be caused by the attachment of bacteria onto kaolinite, which was adsorbed onto the solid matrix.